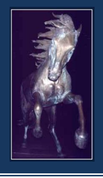

Comparison of Bioluminescence and Fluorescence Imaging as Tools for Evaluating Growth of MCF7 and 4T1 Mammary Tumors

Elisa B. Lin, Alex Winters, Jeni Gerberich, Trey Campbell, Li Liu, Devin O'Kelly, Ralph P. Mason*

Department of Radiology, University of Texas Southwestern Medical Center, Dallas, Texas 75390, United States

UTSouthwestern Medical Center

Introduction

- Tumor growth can be assessed by a variety of small animal imaging modalities which are cheap, easy, and efficient.[1] In particular, two optical imaging modalities, bioluminescence imaging (BLI) and fluorescence imaging (FLI), have received attention for their ability to measure tumor growth and response to treatment.[2]
- Both imaging modalities are accurate and well established, however, each method has its own unique advantages and limitations.[1,2]
- BLI has been proven to be inexpensive, to provide high throughput analysis, and to be non-invasive. However, it is impacted by the uniformity of charge-coupled device camera detection.[3]
- FLI, unlike BLI, does not depend on administration of luciferin, but it could potentially underestimate deep signal changes.[3]

- In this study, caliper measured volume is considered to be the gold standard and the reference to which optical imaging is compared.
- This study compared the use of BLI and FLI to characterize and monitor growth of mammary 4T1-luc and MCF7-luc-GFP-mCherry tumors in nude mice.

Methods

General Considerations

- Orthotopic mammary fat pad tumors, ~1 million cells each:
  - 3 4T1-luc mice (R1, R2, R3) were imaged using BLI over 3 days.
  - 3 4T1-luc cells (L1R1, L1R2, L1R3) mice were imaged using BLI over 22 days.
  - 3 MCF7-luc-GFP-mCherry mice (L1, L2, L3) were imaged using FLI and BLI over 18 days.
  - 3 MCF7-luc-GFP-mCherry mice (L2R1, L2R2, L3R1) were imaged using FLI and BLI for an additional 19 days.

- Mice were anesthetized with isoflurane and oxygen.
- Volume measurements were taken with electronic calipers immediately after the conclusion of each imaging sequence.

BLI – 4T1-luc and MCF7-luc-GFP-mCherry tumors.

- Sodium *D*-luciferin (80 µL, 40 mg/mL, Gold Biotechnology, St. Louis, MO) was injected subcutaneously in the fore-back neck region.

- Image sequences were collected for 20 minutes using the IVIS® Spectrum (1 minute delay between each image, camera aperture (f-stop) = 1, binning = "small").
  - Selected exposure time was kept constant for each sequence (varied from day to day).
    - Before each sequence was collected, a single image was taken with auto exposure; the value selected was set manually for each BLI sequence.

- Methods used to evaluate the results of the BLI experiments:
  - "Max" values were taken at the maximum observed BLI signal at any time point.
  - "10 min" values were taken exactly at the 10 minute mark of each sequence, regardless of when the injection was actually given.
  - "Area under the curve" (AUC) values were calculated by using the trapezoid method across all available time points, to give a value that was less sensitive to temporal inaccuracies.

FLI – MCF7-luc-GFP-mCherry tumors.

- Image sequences were collected using the IVIS® Spectrum (camera aperture (f-stop) = 1, pixel binning = 8).
  - Images were collected using the system's "auto exposure" feature, to ensure each image received a sufficient amount of light for spectral unmixing.
  - Optimal detection of mCherry, based off of maximum fluorescence signal, was achieved with λ_{ex} = 570 nm and λ_{em} = 620 nm.
  - Excitation and emission filters were chosen to ensure spectral range would adequately cover the peaks for both dyes (GFP and mCherry).

- Methods used to evaluate the results of the FLI experiments:
  - The "single wavelength" method involved selecting the image with excitation/emission filters that most closely hit the peak of the dye in question, followed by region of interest (ROI) analysis of the tumor in a manner similar to the BLI analysis done earlier.
  - AUC analysis values were calculated by using the trapezoid method for each filter pair.
    - Note: this analysis "integrates" over frequency space as opposed to time space. Both, however, offer a value that can help quantify the strength of a BLI/FLI experiment over the entire area, instead of just at one particular point.

Graphs – BLI and FLI

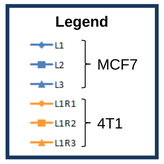

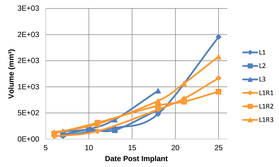

Figure 1. Volume vs. Date

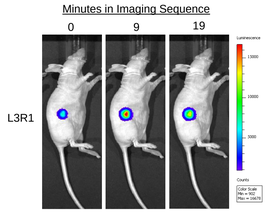

Figure 2. Dynamic BLI of mouse L3R1 at 0, 9, and 19 minutes into the imaging sequence.

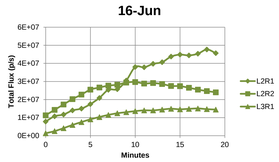

Figure 3. Example of dynamic BLI curves. Data points are derived from images like the ones shown in Figure 2.

- Representatives of each tumor type were chosen to be displayed.
- As expected, the growth of volume as measured by caliper showed a continuously rising and exponential trend.
- An example of a dynamic BLI curve is shown (Figure 3) as the subsequent BLI graphs are derived from these curves.
- Peak of BLI signal was typically between 15-20 minutes.

FLI Graphs

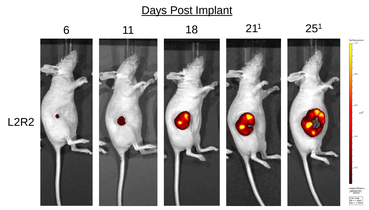

Figure 4. FLI of mouse L2R2 at 6, 11, 18, 21, and 25 days post implant. Images are taken at λ_{ex} = 570 nm and λ_{em} = 620 nm.

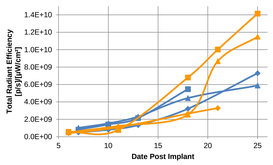

Figure 5. FLI Total Radiant Efficiency vs. Date

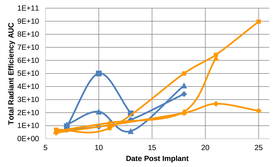

Figure 6. FLI Total Radiant Efficiency AUC vs. Date

- Data in figures 5 and 6 was derived from images like the type shown in Figure 4.
- AUC took into consideration the entire FLI sequence, as opposed to the radiant efficiency at one point (one excitation filter, one emission filter). However, the AUC curves showed less of an exponential growth trend.
- [1]Abscence of red signal in the center is from scarring blocking the FLI signal.

BLI Graphs

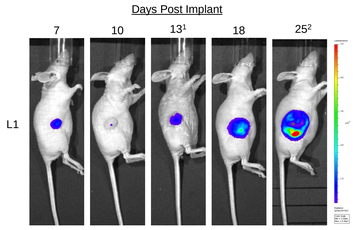

Figure 7. BLI images of mouse L1 at 7, 10, 13, 18, and 25 days post implant. Images are chosen from the maximum values in each sequence.

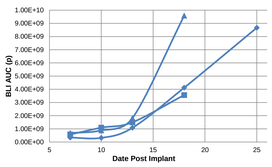

Figure 9. BLI AUC vs. Date (MCF7). Data is derived from images like the type shown in Figure 7.

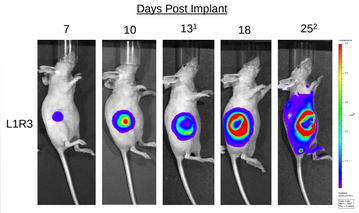

Figure 8. BLI images of mouse L1R3 at 6, 11, 18, 21, and 25 days post implant. Images are chosen from the maximum values in each sequence.

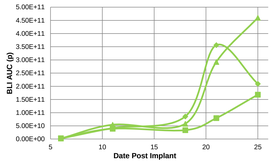

Figure 10. BLI AUC vs. Date (4T1). Data is derived from images like the type shown in Figure 8.

- Total flux (p/s) values from ROI's placed on the tumor for each image allowed observation of BLI signal growth versus time through each session and each day.
- BLI showed steady growth of signal in Figure 7, with an inexplicable drop at 10 days post implant that contradicts caliper measurements.
- BLI showed steady growth of signal in Figure 8, as expected.
- [1]13 days post implant, a *C. bovis* infection can be seen (it was treated upon recognition).
- [2]25 days post implant, notable scarring obscures BLI signal.

BLI vs. FLI Graphs

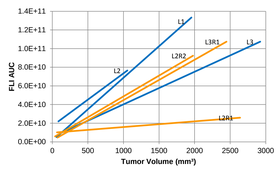

Figure 11. FLI AUC vs. Volume. Growth of FLI AUC data with volume showed similar behavior for most mice.

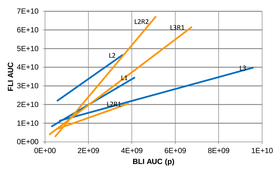

Figure 12. FLI AUC vs. BLI AUC. FLI and BLI showed strong similarities for small tumors/weak signals. Differences increased as tumors grew and scarring developed.

- No significant advantages or disadvantages were observed between "max" and "10 min" values (not shown) when graphed against time and caliper-measured tumor volume.
- Analysis of data using the AUC method showed similar trends amongst the available data when compared while analyzing only at the maximum BLI or FLI value.

Conclusion Graphs

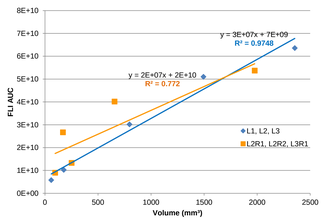

Figure 13. FLI AUC vs. Volume (MCF7, Grouped by Date of Implant)

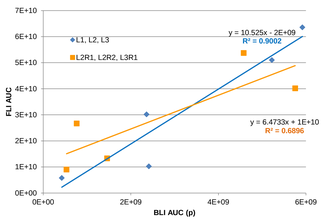

Figure 14. FLI AUC vs. BLI AUC (MCF7, Grouped by Date of Implant)

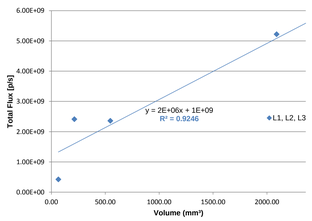

Figure 15. BLI AUC vs Volume (MCF7, Grouped)

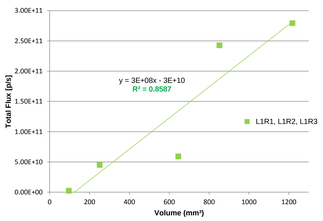

Figure 16. BLI AUC vs Volume (4T1, Grouped)

Graphs – Metastases

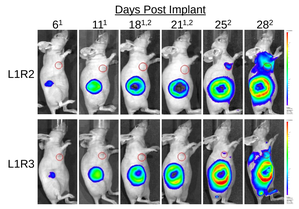

Figure 17. BLI images of mice L1R2 and L1R3 at 6, 11, 18, 21, 25, and 28 days post implant

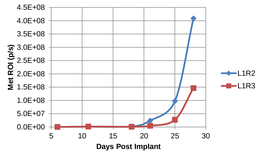

Figure 18. Integrated total photon flux (p/s) versus date

- As expected, BLI grows continuously and exponentially over time.
- [1]Metastases here are sub-palpable, but as seen in figures 18 and 19, can be detected by BLI.
- [2]Notable scarring here is shown as a ring within the center of the BLI signal.

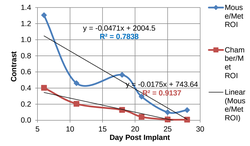

Figure 19. Comparison of metastases signal strength with the imaging chamber and tumor-free tissue

Discussion

- The AUC method greatly simplified the imaging workflow and removed the need for perfect temporal accuracy, since all times and wavelengths were considered.
- BLI showed strong correlation with tumor volume (R^2 = *0.92 and 0.86, for MCF7 and 4T1, respectively*) (Figures 15-16).
- FLI showed strong correlation with tumor volume (R^2 = *0.97 and 0.77*) (Figure 13).
- BLI and FLI signals were correlated (R^2 = *0.90 and 0.69)* (Figures 14).

- Experimental difficulties like tumor scarring and a mid-experiment *C. bovis* infection compromised data quality (Figures 4, 7, 8, 17).
- Strong correlations were established between BLI, FLI, and tumor volume, providing evidence that each method could be used to validate the other and reduce overall error.

Conclusion

Specific benefits of BLI and FLI

- BLI allows detection of sub-palpable tumors at deeper volumes and additional metastases.
  - Caliper measurements are simple only for subcutaneous tumors.
- BLI offers particularly strong contrast to noise, but requires the administration of luciferin substrate.
- FLI signal is subject to background auto fluorescence.
  - This became a particular problem when the *C. bovis* infection occurred.
- Caliper measurement was not as useful for measuring small tumor volumes due to the possible interference of thick skin. However, BLI was not as useful for the measurements of large tumor volumes due to tumor scarring.

- The investigations to date largely confirm growth characteristics and the utility of available imaging methods matching the extant literature.
- The correlations, which had not been examined for 4T1-luc tumors at UTSW previously, provide a foundation for my forthcoming medical school research activity.
- Future plans include continued investigation of metastases and utilizing Multispectral Optoacoustic Tomography (MSOT) for integrated hypoxia studies.

References

(1) Alhasan MK, Liu L, Lewis MA, Magnusson J, Mason RP. Comparison of Optical and Power Doppler Ultrasound Imaging for Non-Invasive Evaluation of Arsenic Trioxide as a Vascular Disrupting Agent in Tumors. *PLoS ONE* 2012; 7(9): 1-9.

(2) Choy G, O'Connor S, Diehn FE, Costouros N, Alexander HR, Choyke P, Libutti SK. Comparison of noninvasive fluorescent and bioluminescent small animal optical imaging. *Biotechniques* 2003; 35(5): 1022-1030.

(3) Liu L, Mason RP, Gimi B. Dynamic bioluminescence and fluorescence imaging of the effects of the antivascular agent Combretastatin-A4P (CA4P) on brain tumor xenografts. *Elsevier* 2014; 356(2):1-8.

Acknowledgments

This work was supported in part by the University of Texas Southwestern Medical Center Radiology Department and in part by the Cancer Prevention and Research Institute of Texas (CPRIT, Grant No. RP140399) in collaboration with Drs. Kevin Pinney and Mary Lynn Trawick, Baylor University. Imaging was facilitated by the Southwestern Small Animal Imaging Resource, which was supported in part by the NIH Comprehensive Cancer Center Grant P30 CA142543 and a Shared Instrumentation Grant 1S10 RR024757. I thank Jeni Gerberich and Dr. Li Liu for the preparation of cell lines. I thank Alex Winters, Trey Campbell, and Devin O'Kelly for their mentorship and endless patience and wisdom in this entire endeavor. I thank Dr. Mo Yang and Jo Wagner for providing a wonderful work environment. I thank Dr. Ralph Mason as a principal investigator and for his guidance and insight into appropriate topics of study.